Supplementary Information

Build-up and Decay of the Optical Absorption in the Ultrafast Generation and Reaction of Benzhydryl Cations in Solution

Benjamin P. Fingerhut,[a,§] *Christian F. Sailer,*[b] *Johannes Ammer,*[a]

*Eberhard Riedle,**[b] *and Regina de Vivie-Riedle**[a]

[a] Department Chemie, Ludwig-Maximilians-Universität (LMU), Butenandt-Str. 11, 81377 München, Germany.

[b] Lehrstuhl für BioMolekulare Optik, Ludwig-Maximilians-Universität (LMU), Oettingenstr. 67, 80538 München, Germany.

* Corresponding author: E-mail: Riedle@physik.uni-muenchen.de

Regina.de_Vivie@cup.uni-muenchen.de

§ Current address:

Department of Chemistry, University of California, Irvine, California 92697-2025, USA

E-mail: bfingerh@uci.edu

1 Materials

The solvents used were of the highest spectroscopic grade available. Benzhydryl chloride (Ph_2CHCl) was purchased from Sigma-Aldrich and used without further purification. The derivatives $(tol)_2CHCl$ and mfp(Ph)CHCl were prepared as described in references [2, 3]. The synthesis of $tol(Ph)CH\text{-}PPh_3^+\ BF_4^-$ and $(mfp)_2CH\text{-}PPh_3^+\ BF_4^-$ will be reported elsewhere.

3,3',5-Trifluorobenzhydryl chloride dfp(mfp)CHCl was obtained from thionyl chloride (1.3 mL, 18 mmol) and 3,3',5-trifluorobenzhydrol (dfp(mfp)CHOH) [3] (3.00 g, 12.6 mmol) in dichloromethane (10 mL). The crude product was distilled in the vacuum (196–198 °C / 1.1×10^{-2} mbar) to give a colorless oil (2.3 g, 72 %).

^{1}H NMR (300 MHz, $CDCl_3$): δ = 5.98 (s, 1 H, CHCl), 6.74 (tt, $^3J_{HF}$ = 8.7 Hz, $^4J_{HH}$ = 2.3 Hz, 1 H, 4-ArH), 6.89-7.04 (m, 3 H, ArH), 7.08-7.16 (m, 2 H, ArH), 7.28-7.35 ppm. (m, 1 H, ArH);

^{13}C NMR {^{1}H}(75.5 MHz, $CDCl_3$): δ = 61.8 (td, $^4J_{CF}$ = 2.3 Hz, $^4J_{CF}$ = 2.1 Hz, CHCl), 103.8 (t, $^2J_{CF}$ = 25.3 Hz, 4-Ar), 110.7–111.1 (m, AXX'-system, 2,6-Ar), 114.9 (d, $^2J_{CF}$ = 23.0 Hz, 2'-Ar or 4'-Ar), 115.7 (d, $^2J_{CF}$ = 21.2 Hz, 2'-Ar or 4'-Ar), 123.3 (d, $^4J_{CF}$ = 3.0 Hz, 6'-Ar), 130.4 (d, $^3J_{CF}$ = 8.3 Hz, 5'-Ar), 142.3 (d, $^3J_{CF}$ = 7.2 Hz, 1'-Ar), 144.2 (t, $^3J_{CF}$ = 9.0 Hz, 1-Ar), 162.8 (d, $^1J_{CF}$ = 247.5 Hz, 3'-Ar), 163.0 ppm. (dd, $^1J_{CF}$ = 249.4 Hz, $^3J_{CF}$ = 12.1 Hz, 3,5-Ar);

^{19}F-NMR (282 MHz, $CDCl_3$): −108.4 - −108.5 ppm. (m, 3,5-F); −111.6 (m, 3'-F);

MS (+EI): m/z (%) = 256.1 (3) [M^+], 237.2 (4) 222.2 (36), 221.1 (100) [$M-Cl^-$], 219.1 (34), 201.1 (35);

Anal. calcd. for $C_{13}H_8ClF_3$: C, 60.84; H, 3.14. Found: C, 60.61; H, 3.16.

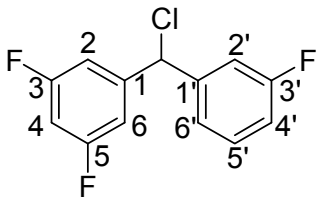

2 Theoretical concepts

We summarize the theoretical methods for the microsolvation approach. Different quantum chemical methods are used to obtain accurate ground state geometries, which are needed to generate the initial conditions for the on-the-fly MD simulations. We consider the solvation dynamics, the intramolecular relaxation and the electrophile-nucleophile bond formation. With appropriate correlation functions we analyze the relaxation process and quantify the accuracy of the microsolvation approach.

On-the-fly Molecular Dynamics (MD)

The dynamics of the nascent microsolvated benzhydryl cation (designated as model system MS_{start}) is simulated by on-the-fly MD. The method requires an energy and a gradient calculation of the MS_{start} on the respective level of theory at every time-step (Δt = 1 fs), but avoids the construction of global potential energy surfaces. In all dynamics simulations energies and gradients are calculated on the RI-BLYP-D level of theory [4-10] with the parallel version of the Turbomole program package [11]. The accuracy of the RI-BLYP-D method is tested against different functionals and MP2 as a wave function based method which inherently includes the dispersion interaction (for details see below). The resulting equations of motion of the nuclei are calculated with the Newton-X package [12]. Time integration is performed with the velocity-verlet algorithm [13].

Initial conditions. The non-equilibrium start geometries MS_{start} for the on-the-fly MD simulations that mimic the nascent microsolvated benzhydryl cation are generated by breaking the bond between the central methyl carbon and the phosphor atom in the phosphine leaving group (C^1-P bond) in $(dfp)_2CH\text{-}P^+(CH_3)_3$ with all other degrees of freedom frozen in the precursor cluster (PC: $(dfp)_2CH\text{-}P^+(CH_3)_3 \bullet XCH_3OH$) equilibrium geometry. The leaving group $P(CH_3)_3$ is placed at a distance of 5.0 Å from the central C^1-Atom (see Fig. 1). According to the best available knowledge [14-16] we assume that the ultrafast bond cleavage (fs-ps) proceeds faster than the intramolecular relaxation. The initial velocities are generated by depositing the excitation energy of an assumed pump pulse $E_{h\nu}$ = 4.8 eV (λ = 258 nm) as kinetic energy equally in all degrees of freedom [17] in the MS_{start}. The error due to the neglect of the ground state dissociation enthalpy is estimated to be only 10 % [18]. A Gaussian distributed random number is assigned as initial velocity v_i to every atom i. After

removing the center of mass translation and rotation, the kinetic energy of atom i can be rescaled according to

$$v_i^{ini} = \sqrt{\frac{2E_{Kin}}{\sum_k M_k v_k^2}} v_i, \quad \text{for} \quad k \neq i \qquad (1)$$

where M_k is the mass of all other atoms k. The Gaussian distributed initial velocities v^{ini}_i describe the non-equilibrium ensemble subsequent to photolysis and not a canonical ensemble under equilibrium conditions.

This velocity distribution (vs. Wigner) is motivated by the ultrafast bond cleavage. Due to the dissociative character of the excited state potential energy surface most of the excitation energy is directly converted into kinetic energy of the dissociating fragments within 200 fs [16]. In the liquid phase the fragments are confined in the first solvation shell and kinetic energy is transferred by elastic scattering from the solute to solvent molecules. In this work the subsequent redistribution within the solute and solvent vibrational modes is investigated. The total simulation time of the individual trajectories is 4 ps (time step Δt = 1fs). For the given initial conditions a total of 45 independent trajectories $\{MS_i(0)\}$ (i = 1, 2, … 45) are generated. The considered bond formation reaction of the benzhydryl cation obeys a single reaction channel which makes the statistical discrimination and assignment of branching ratios, typically requiring many trajectories [19, 20], unnecessary. All 45 trajectories lead to a bond formation within 4 ps. The statistical acceptability for the temporal evolution is tested against experimental observable correlation functions and spectra (see Results and Discussion).

Quantum chemical methods. The electronic Schrödinger equation, required to be evaluated in every time step, is solved on the DFT level of theory [4, 5] within the resolution of the identity approximation [6], including empirical dispersive energy correction (RI-DFT-D) [7, 8]. All calculations are done with the Turbomole program package [11] using a split valence double zeta basis set (def-SV(P)). The Coulomb 2-el integrals are evaluated within the resolution of the identity approximation [6], where an auxiliary def-TZVP basis is used. Regarding the choice of the basis set, one could argue that the limited def-SV(P) is inadequate to properly describe excited states; however, the main interest here is the simulation of geometrical changes in the ground state and the analysis of excited states is limited to valence

states π - π^* (see below), for which the use of larger basis sets including diffuse functions should not be necessary [21, 22].

The B-LYP functional [9, 10] is used to obtain reliable equilibrium geometries, gradients and potential energy curvatures (i.e. harmonic frequencies) [23] probably due to systematic error compensation [24-27]. We optimized a reference cluster (RC) consisting of the precursor molecule $Ph_2CH\text{-}P^+(CH_3)_3$ and four methanol molecules (RC: DPM-$P^+(CH_3)_3$ • $4CH_3OH$, 57 atoms). The moderate size of the cluster allows to test the accuracy of the quantum chemical method against other functionals (RI-BLYP-D [4-10] vs. RI-BLYP [4-6, 9, 10] vs. tpss [28, 29] vs. M06-HF [30, 31]) and to estimate the importance of the dispersion correction. Further reference calculations with wave function based methods (RI-MP2) [32-34], which inherently include the intermolecular interactions, were also performed.

Based on this comparison, RI-BLYP-D is selected to determine how many methanol (CH_3OH) molecules are needed to complete the first solvation shell. In order to reduce the MD simulation time, the more reactive tetra-fluoro derivate $(dfp)_2CH\text{-}P^+(CH_3)_3$ rather than $Ph_2CH\text{-}P^+(CH_3)_3$ was chosen as precursor molecule. Two different precursor clusters (PC), one surrounded by eight methanol molecules (PC1: $(dfp)_2CH\text{-}P^+(CH_3)_3$ • $8CH_3OH$, 85 atoms) and one surrounded by nine methanol molecules (PC2: $(dfp)_2CH\text{-}P^+(CH_3)_3$ • $9CH_3OH$, 90 atoms) are optimized as reference geometry for the molecular dynamics simulations. The choice of two different precursor clusters accounts for the fact that a first solvation shell is not uniquely defined and can take up more than one configuration. The CPU-requirement for a combined energy and gradient calculation of the PC's at each time-step is on the order of two minutes on eight processors of a modern linux cluster. This allows for a dynamic description of the electrophile-nucleophile bond formation reaction in on-the-fly MD simulations up to a ps timescale.

The electronically excited π– π^* states of the micro-solvated $(dfp)_2CH^+$ cation are needed along the on-the-fly MD trajectories to evaluate the time resolved UV-VIS spectra $S_{UV-VIS}(t,\lambda)$. The excitation energies and transition moments are calculated by TD-DFT calculations [35-37] at the evaluated geometries. Though the B-LYP functional neglects non-local exchange the used methodology has been shown previously to yield reasonable results for excitation energies [38] owing to fortuitous cancelation of errors [24]. Abundant excited charge transfer (CT) states suffer from electron transfer self-interaction in TD-DFT, resulting in too low excitation energies of the spurious CT states [39, 40]. Here they are discarded in

the discussion of the locally excited π - π* valence state of $(dfp)_2CH^+$ (characterized by the HOMO-LUMO single excitation).

Model compounds for microsolvation

A reference cluster (RC) consisting of the precursor molecule $Ph_2CH\text{-}P_+(CH_3)_3$ surrounded by four methanol molecules is used as a benchmark for the ab initio method appropriate for the larger precursor clusters (PC1 and PC2). The moderate cluster size allows the optimization of the equilibrium geometry of the RC with different functionals (tpss, RI-BLYP, RI-BLYP-D, M06-HF) and at a wave function based level of theory (RI-MP2). RI-MP2 serves as reference method for the intermolecular interactions as they are inherently included. All equilibrium geometries are confirmed by normal mode analysis and are summarized in Table 1.

The hydrogen bond network (upper block in Table 1) is of similar strength in all DFT based methods, but the bonds are slightly shorter than in the RI-MP2 optimized minimum. The inter-solvent C-C distances ($C_{CH_3OH} - C_{CH_3OH}$, middle block in Table 1) obtained from traditional DFT methods differ substantially from the RI-MP2 results, which show much shorter $C_{CH_3OH} - C_{CH_3OH}$ - distances ($\Delta r = 0.2$ Å for the minimal distances). This error can be eliminated by the dispersion corrected functional RI-BLYP-D indicating that traditional DFT methods underestimate the non-polar C-C interaction of the hydrogen bonded solvent. $C_{CH_3OH} - C_{CH_3OH}$ - distances calculated with the hybrid meta-GGA functional M06-HF are similar to the RI-BLYP-D values. The binding interaction between solute and solvent are described well by the RI-MP2 and the RI-BLYP-D calculations as visible in similar mean values for $C^1 - O_{CH_3OH}$ distances (lower block in Table 1). Again traditional DFT underestimates this solute-solvent interaction. As a consequence we selected the RI-BLYP-D method as best compromise between accuracy and computational efficiency to optimize the PC's.

The PC is designed as a precursor molecule $(dfp)_2CH\text{-}P^+(CH_3)_3$ surrounded by a first solvation shell. We find that eight to nine CH_3OH molecules are required to close the first shell. The large variances of the $C^1 - O_{CH_3OH}$ solute-solvent distances in the PC equilibrium geometries (see lower block in Table 1), compared to the RC geometries are a result of surface crowding effects. Due to steric hindrance not all solvent molecules can cover the solute simultaneously. Between themselves the solvent molecules form a pronounced inter-solvent hydrogen bond network, the coordination towards the F-atoms is only weakly

developed. Furthermore our calculations show that already the solvation of a charged solute in the polar solvent CH_3OH ($\varepsilon = 32.63$, dipole-moment = 1.77 debye) requires the dispersion interaction to be considered besides the dipolar interaction. Otherwise over-binding within the hydrogen-bond network is observed, at the cost of the solute-solvent interaction.

3 References

[1] Megerle, U.; Pugliesi, I.; Schriever, C.; Sailer, C. F.; Riedle, E. *Appl. Phys. B* **2009**, *96*, 215-231.

[2] Denegri, B.; Streiter, A.; Jurić, S.; Ofial, A. R.; Kronja, O.; Mayr, H. *Chem. Eur. J.* **2006,** *12*, 1648-1656.

[3] Nolte, C.; Mayr, H. *Eur. J. Org. Chem.* **2010**, 1435-1439.

[4] Treutler, O.; Ahlrichs, R. *J. Chem. Phys.* **1995**, *102*, 346-354.

[5] von Arnim, M.; Ahlrichs, R. *J. Comput. Chem.* **1998**, *19*, 1746-1746.

[6] Eichkorn, K.; Weigend, F.; Treutler, O.; Ahlrichs, R. *Theo. Chem. Acc.* **1997**, *97*, 119-124.

[7] Grimme, S. *J. Comput. Chem.* **2004**, *25*, 1463-1473.

[8] Grimme, S. *J. Comput. Chem.* **2006**, *27*, 1787-1799.

[9] Becke, A. D. *Phys. Rev. A* **1988**, *38*, 3098-3100.

[10] Lee, C.; Yang, W.; Parr, R..G. *Phys. Rev. B* **1988**, *37*, 785-789.

[11] Ahlrichs, R.; Bär, M.; Häser, M.; Horn, H.; Kölmel, C. *Chem. Phys. Lett.* **1989**, *162*, 165-169.

[12] Barbatti, M.; Granucci, G.; Persico, M.; Ruckenbauer, M.; Vazdar, M.; Eckert-Maksić, M.; Lischka, H. *J. Photochem. Photobiol. A* **2007**, *190*, 228-240.

[13] Swope, W. C.; Andersen, H. C.; Berens, P. H.; Wilson, K. R. *J. Chem. Phys.* **1982**, *76*, 637.

[14] Peters, K. S. *Chem. Rev.* **2007**, *107*, 859-873.

[15] Lipson, M.; Deniz, A. A.; Peters, K. S. *J. Am. Chem. Soc.* **1996**, *118*, 2992-2997.

[16] Fingerhut, B. P.; Geppert, D.; de Vivie-Riedle, R. *Chem. Phys.* **2008**, *343*, 329-339.

[17] Sellner, B.; Barbatti, M.; Lischka, H. *J. Chem. Phys.* **2009**, *131*, 024312.

[18] Bartl, J.; Steenken, S.; Mayr, H.; McClelland, R. A. *J. Am. Chem. Soc*. **1990**, *112*, 6918-6928.

[19] Tachikawa, H.; Igarashi, M.; Ishibashi, T. *Chem. Phys. Lett.* **2002**, *363*, 355-361.

[20] Rudić, S.; Murray, C.; Harvey, J. N.; Orr-Ewing, A. J. *J. Chem. Phys.* **2004**, *120*, 186-198.

[21] Scalmani, G.; Frisch, M. J.; Mennucci, B.; Tomasi, J.; Cammi, R.; Barone, V. *J. Chem. Phys.*. **2006**, *124*, 94107.

[22] Cammi, R.; Mennucci, B.; Tomasi, J. *J. Phys. Chem. A*. **2000**, *104*, 5631-5637.

[23] Zhao, Y.; Truhlar, D. G. *Theo. Chem. Account*. **2008**, *120*, 215-241.

[24] Dreuw, A.; Harbach, P. H. P.; Mewes, J. M.; Wormit, M. *Theor. Chem. Acc.* **2010**, *125*, 419–426.

[25] Zhou, Z.; Du, D.; Fu, A.; Yu, Q. *THEOCHEM* **2000**, *530*, 149-154.

[26] Prall, M.; Wittkopp, A.; Fokin, A. A.; Schreiner, P. R. *J. Comput. Chem.* **2001**, *22*, 1605-1614.

[27] Kraka, E.; Cremer, D. *J.* Am. *Chem. Soc.* **2000**, *122*, 8245-8264.

[28] Perdew, J. P.; Wang, J. *Phys. Rev. B* **1992**, *45*, 13244-13249.

[29] Tao, J.; Perdew, J. P.; Staroverov, V. N.; Scuseria, G. E. *Phys. Rev. Lett.* **2003**, *91*, 146401-146404.

[30] Zhao, Y.; Truhlar, D. G. *J. Phys. Chem. A* **2006**, *110*, 13126-30.

[31] Gaussian 09, R. A., M. J. Frisch, G. W. Trucks, H. B. Schlegel, G. E. Scuseria, M. A. Robb, J. R. Cheeseman, G. Scalmani, V. Barone, B. Mennucci, G. A. Petersson, H. Nakatsuji, M. Caricato, X. Li, H. P. Hratchian, A. F. Izmaylov, J. Bloino, G. Zheng, J. L. Sonnenberg, M. Hada, M. Ehara, K. Toyota, R. Fukuda, J. Hasegawa, M. Ishida, T. Nakajima, Y. Honda, O. Kitao, H. Nakai, T. Vreven, J. A. Montgomery, Jr., J. E. Peralta, F. Ogliaro, M. Bearpark, J. J. Heyd, E. Brothers, K. N. Kudin, V. N. Staroverov, R. Kobayashi, J. Normand, K. Raghavachari, A. Rendell, J. C. Burant, S. S. Iyengar, J. Tomasi, M. Cossi, N. Rega, J. M. Millam, M. Klene, J. E. Knox, J. B. Cross, V. Bakken, C. Adamo, J. Jaramillo, R. Gomperts, R. E. Stratmann, O. Yazyev, A. J. Austin, R. Cammi, C. Pomelli, J. W. Ochterski, R. L. Martin, K. Morokuma, V. G. Zakrzewski, G. A. Voth, P. Salvador, J. J. Dannenberg, S. Dapprich, A. D. Daniels, Ö. Farkas, J. B. Foresman, J. V. Ortiz, J. Cioslowski, and D. J. Fox, Gaussian, Inc.. Wallingford CT: 2009.

[32] Hättig, C.; Weigend, F. *J. Chem. Phys.* **2000**, *113*, 5154.

[33] Hättig, C. *J. Chem.* Phys. **2003**, *118*, 7751.

[34] Hättig, C.; Hellweg, A.; Köhn, A. *Phys. Chem. Chem. Phys.* **2006**, *8*, 1159-1169.

[35] Furche, F.; Rappoport, D. *Theo. Comput. Chem.* **2005**, *16*, 93-128.

[36] Bauernschmitt, R.; Häser, M.; Treutler, O.; Ahlrichs, R. *Chem. Phys. Lett.* **1997**, *264*, 573-578.

[37] Bauernschmitt, R.; Ahlrichs, R. *Chem. Phys. Lett.* **1996**, *256*, 454-464.

[38] Dreuw, A.; Weisman, J. L.; Head-Gordon, M. *J. Chem. Phys.*. **2003**, *119*, 2943.

[39] Starcke, J. H.; Wormit, M.; Schirmer, J.; Dreuw, A. *Chem. Phys.*. **2006**, *329*, 39-49.

[40] Dreuw, A. *Chem.Phys.Chem.* **2006**, *7*, 2259-2274.

Table 1: (next page)

Calculated hydrogen bonds (r(O···H)), inter-solvent C-C distances ($C_{CH_3OH} - C_{CH_3OH}$) and solute C^1 - solvent O_{CH_3OH} distances ($C^1 - O_{CH_3OH}$) in the optimized reference cluster (RC) geometries $Ph_2CH\text{-}P^+(CH_3)_3 \cdot 4\ CH_3OH$ and in the optimized precursor cluster (PC) geometries (PC1 = $(dfp)_2CH\text{-}P^+(CH_3)_3 \cdot 8\ CH_3OH$, PC2 = $(dfp)_2CH\text{-}P^+(CH_3)_3 \cdot 9\ CH_3OH$). Basis: def-SV(P), aug:def-TZVP, for the M06-HF functional the comparable basis 6-31G* was used; the optimized precursor cluster (PC) geometries PC1 and PC2 are starting clusters for the on-the-fly MD trajectories. All bond lengths are given in [Å].

method	**r(O···H)max**	**r(O···H)min**	**mean**
RC:			
tpss	1.677	1.628	1.654
BLYP	1.702	1.647	1.675
RI-BLYP-D	1.688	1.617	1.650
RI-MP2	1.743	1.654	1.705
M06-HF	1.807	1.762	1.777
PC:			
RI-BLYP-D (PC1)	1.745	1.699	1.717
RI-BLYP-D (PC2)	1.736	1.601	1.660
RC:	r($C_{CH_3OH} - C_{CH_3OH}$) **max**	r($C_{CH_3OH} - C_{CH_3OH}$) **min**	mean
tpss	4.247	4.141	4.210
BLYP	4.277	4.237	4.254
RI-BLYP-D	4.286	3.810	4.029
RI-MP2	4.184	3.970	4.100
M06-HF	4.690	3.881	4.229
PC:			
RI-BLYP-D (PC1)	4.264	3.442	3.955
RI-BLYP-D (PC2)	4.337	3.563	4.101
RC:	r($C^1 - O_{CH_3OH}$)max	r($C^1 - O_{CH_3OH}$)min	mean
tpss	4.251	3.566	3.988
BLYP	4.351	3.383	4.026
RI-BLYP-D	4.035	3.188	3.549
RI-MP2	4.010	3.312	3.555
M06-HF	3.941	3.183	3.584
PC:			
RI-BLYP-D (PC1)	5.458	3.090	4.607
RI-BLYP-D (PC2)	5.327	3.096	4.450